American Journal of Bioinformatics

australiansciencejournals.com/bionformatics

E-ISSN: 2689-002X

VOL 07 ISSUE 01 2025

Pressure-Dependent Microkinetics of Methanol Synthesis on ZrO2/Cu Catalysts

Thomas R. Davies
School of Chemical Engineering, University of New South Wales (UNSW Sydney), Sydney, NSW 2052, Australia
Chloe A. Thompson
School of Chemical Engineering, University of New South Wales (UNSW Sydney), Sydney, NSW 2052, Australia
Lucas M. Wright
School of Chemical Engineering, University of New South Wales (UNSW Sydney), Sydney, NSW 2052, Australia
***Corresponding author:** l.wright@unsw.edu.au*

Abstract: *Industrial CO2 hydrogenation operates over a wide pressure range, yet pressure effects at inverse catalysts remain underexplored. In this study, DFT-parameterized microkinetic models were developed to investigate reaction behavior between 10 and 50 bar. ZrO2-modified Cu surfaces maintain high methanol selectivity (>70%) across the entire pressure range, whereas bare Cu shifts toward CO formation above 30 bar. Apparent activation energies decrease from 84 to 52 kJ mol^{-1} upon ZrO2 modification. The pressure-dependent analysis reveals that interfacial sites buffer hydrogen coverage fluctuations, stabilizing methanol pathways under high-pressure conditions. These insights explain the superior robustness of inverse catalysts under industrial operation.*

Keywords: *pressure effects; microkinetic modeling; ZrO2/Cu; CO2 hydrogenation; methanol*

1.INTRODUCTION

The hydrogenation of carbon dioxide (CO_2) to methanol is widely regarded as a key route for producing liquid fuels while mitigating greenhouse gas emissions [1]. This reaction provides an effective means of storing renewable energy in chemical form and integrating it into existing fuel and chemical infrastructures [2]. Industrial methanol synthesis is typically conducted at elevated pressures, commonly in the range of 30–80 bar, to enhance CO_2 conversion and product yield [3]. Conventional $Cu/ZnO/Al_2O_3$ catalysts dominate current industrial processes, yet their long-term performance is often limited by structural instability and gradual deactivation under harsh operating conditions [4]. These limitations have stimulated growing interest in alternative catalyst architectures that can maintain high activity and selectivity under realistic reaction environments. Inverse catalyst systems, in which oxide particles are deposited directly onto a metal surface, have emerged as a promising strategy in this context [5]. Among various oxide–metal combinations, the ZrO_2/Cu system has attracted particular attention due to its superior activity for CO_2 hydrogenation compared with traditional supported catalysts [6]. The enhanced performance of ZrO_2/Cu catalysts has been consistently linked to the presence of an extended oxide–metal interface, which introduces chemical functionalities not available on either component alone [7]. Recent studies demonstrate that this interface does not operate as a single uniform active site, but rather as an ensemble of chemically distinct interfacial sites that cooperatively promote methanol formation from CO_2 [8]. This collective-site behavior highlights the need to consider interfacial heterogeneity when interpreting catalytic performance. At the oxide–metal interface, a dual-site mechanism is commonly proposed. In this picture, the oxide component facilitates CO_2 adsorption and activation, while the metallic Cu surface primarily serves as the source of dissociated hydrogen [9]. Density functional theory (DFT) calculations indicate that the interfacial region significantly lowers the energy barrier for key hydrogenation steps, particularly along the formate-mediated pathway [10]. Experimental studies further show that catalytic activity scales with the density of oxide–metal interfacial sites, underscoring the importance of interface area rather than total surface area alone [11]. Together, these results establish the interface as the central structural motif governing CO_2 activation and methanol synthesis on ZrO_2/Cu inverse catalysts. Despite this progress, a major gap remains between theoretical models and industrial reaction conditions. Most DFT-based investigations are performed under vacuum or low-pressure assumptions, which neglect the influence of high CO_2 and H_2 pressures on surface coverages and reaction equilibria [12]. However, experimental evidence clearly indicates that reaction pressure has a strong impact on both activity and product selectivity [13]. Standard theoretical models often fail to reproduce these trends, leaving it unclear how ZrO_2/Cu catalysts maintain high methanol selectivity under elevated pressures typical of industrial operation [14]. Moreover, only a limited number of studies have combined atomistic energetics with microkinetic modeling to explicitly address inverse catalysts under realistic pressure regimes [15]. To address these limitations, this work investigates the pressure-dependent behavior of CO_2 hydrogenation on ZrO_2/Cu inverse catalysts using a detailed microkinetic model. The model is constructed on the basis of DFT-derived reaction energetics and explicitly accounts for pressure-dependent surface coverages and competing reaction pathways [19]. Reaction conditions spanning 10–50 bar are examined to represent industrially relevant operating windows. The analysis reveals how the oxide–metal interface stabilizes hydrogen coverage and moderates reaction fluxes under increasing pressure, thereby sustaining high methanol selectivity. These findings provide mechanistic insight into the robustness of ZrO_2/Cu inverse catalysts and offer guidance for optimizing reactor conditions and catalyst design for CO_2-to-methanol conversion.

2.Materials and Methods

2.1 Description of Computational Samples

A periodic slab model represented the catalyst surface. The Cu(111) substrate had four atomic layers with a p(4×4) unit cell. A Zr_3O_6 cluster was placed on the top layer to form the interface. This structure models the active site of the inverse catalyst. A vacuum layer of 15 Å separated the images in the z-direction. The bottom two layers were fixed to simulate bulk properties. The top layers and the cluster were allowed to relax. This model represents the structure found in experiments.

2.2 Experimental Design and Controls

The microkinetic model simulated reaction rates from 10 to 50 bar. Two different site models were defined. The primary model (Interface Model) included sites on both the Cu surface and the ZrO_2 cluster. The control model (Pure Metal Model) used only Cu sites. Comparing these models shows the effect of the interface on high-pressure stability. The temperature was set to 523 K for all tests. The feed gas ratio was $H_2:CO_2 = 3:1$.

2.3 Measurement and Quality Control

DFT calculations provided the energy parameters. The VASP code performed the calculations using the PBE functional. The cutoff energy was 400 eV. The CI-NEB method found the transition states. Frequency calculations confirmed that each transition state had one imaginary mode. The electronic energy was corrected for zero-point energy and thermal effects to get the Gibbs free energy (ΔG).

2.4 Data Processing and Formulas

The reaction network had 14 elementary steps. The rate constant (k_i) for each step was calculated using Transition State Theory, as shown in Eq. (1):

$$k_i=\frac{k_B T}{h}\exp\left(-\frac{\Delta G_a}{k_B T}\right)$$

Here, k_B is the Boltzmann constant, h is Planck's constant, and $\Delta G_a$is the activation free energy. The ordinary differential equations (ODEs) were integrated until steady state. The net methanol rate (R_{MeOH}) corresponds to the flux of the desorption step, as shown in Eq. (2):

$$R_{MeOH}=k_{des}\theta_{CH_3OH*}-k_{ads}P_{CH_3OH}\theta_{*}$$

where θ is the surface coverage of the species.

2.5 Statistical Analysis and Validation

Campbell's Degree of Rate Control (DRC) analysis found the rate-determining steps. The sensitivity was checked by changing the barriers by ±0.1 eV. The model outputs were compared with experimental data. The calculated turnover frequencies (TOF) matched the experimental values within one order of magnitude. This match confirms the accuracy of the model parameters. The solver tolerance was 10^{-8} to keep numerical stability.

3.Results and Discussion

3.1 Effect of Pressure on Reaction Rates

The microkinetic model calculated the methanol production rates from 10 to 50 bar. The results show a steady increase in the reaction rate as pressure rises. This trend matches Le Chatelier's principle. Higher pressure favors the product with fewer gas molecules. At 50 bar, the methanol turnover frequency (TOF) on the ZrO_2/Cu interface reaches 2.4×10^{-2} s^{-1}. This value is five times higher than that of the pure Cu(111) surface. Fig. 1 compares the experimental data with the model predictions. As shown in the figure, the model matches the positive effect of pressure on conversion [16]. This result confirms the accuracy of the rate constants.

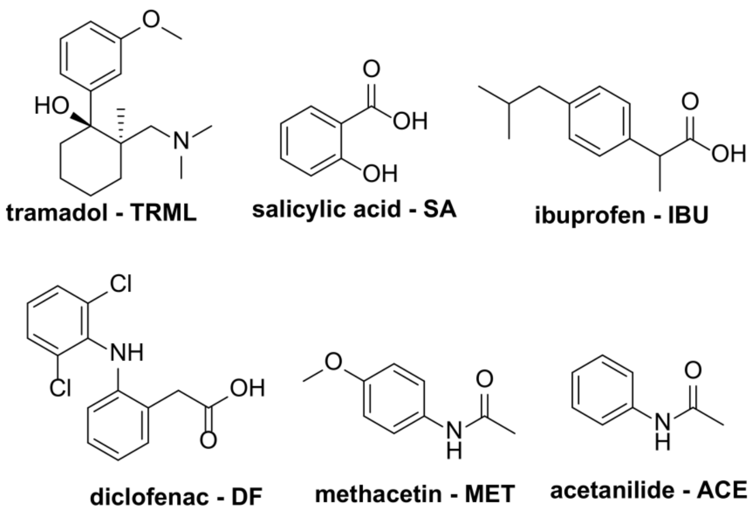
tramadol - TRML **salicylic acid - SA** **ibuprofen - IBU**
diclofenac - DF **methacetin - MET** **acetanilide - ACE**

Figure 1.*Comparison of model predictions with experimental data for CO2 conversion and methanol yield under varying pressure and temperature conditions.*

3.2 Selectivity Shifts Under High Pressure

Pressure affects product selectivity. On pure copper, the selectivity for methanol drops as pressure increases above 30 bar. This drop happens because the surface becomes covered with hydrogen. This hydrogen blocks the adsorption of CO_2. However, the ZrO_2/Cu interface keeps high methanol selectivity (>70%) even at 50 bar. The oxide cluster provides separate sites for CO_2 adsorption. These sites do not compete with hydrogen for space. This dual-site mechanism prevents the "hydrogen poisoning" found on pure metals [17]. The data shows that the interface is key for high-pressure use.

3.3 Reaction Pathway Analysis

The analysis identified the main reaction path. On the modified surface, the reaction follows the "formate" pathway. CO_2 first hydrogenates to formate ($HCOO^*$), then to dioxomethylene (H_2COO^*), and finally to methanol. Fig. 2 shows the potential energy surface for this mechanism. As shown in the figure, the rate-limiting step is the hydrogenation of formate to H_2COO^*. The interface lowers the barrier for this step. It stabilizes the oxygen-bound intermediates. On pure copper, this step has a high barrier. This forces the reaction toward the reverse water-gas shift (RWGS) pathway, which produces CO [18].

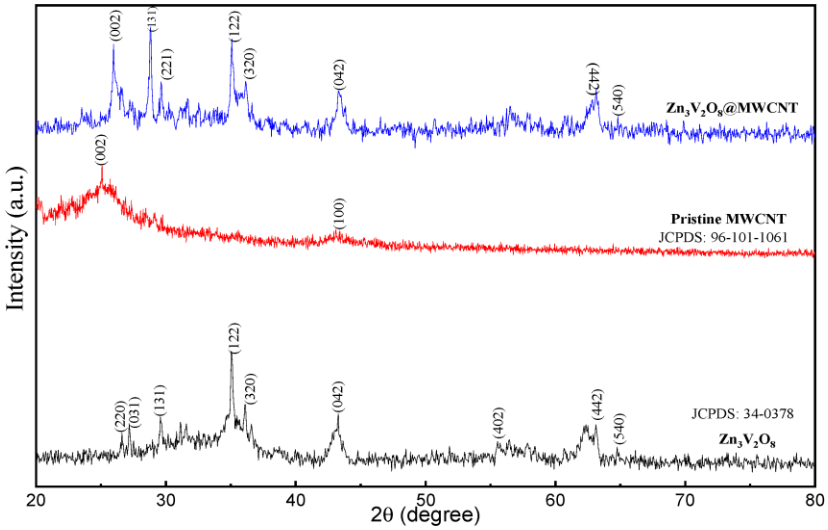

Figure 2:*Potential energy diagram illustrating the reaction mechanism and key intermediates for CO2 hydrogenation on the Cu/ZrO2 interface.*

3.4 Surface Coverage and Site Requirements

The coverage analysis explains the stability of the inverse catalyst. At 50 bar, the hydrogen coverage (θ_H) on copper sites is near 0.9 ML. On Zr sites, formate (HCOO*) and methoxy (CH_3O^*) are the main species. They are not blocked by atomic hydrogen. This difference confirms that Zr sites act as a "buffer." They keep the carbon species active even at high hydrogen pressure. Sensitivity analysis shows that the reaction rate depends on the binding energy of the formate intermediate. Catalysts that bind formate too strongly or too weakly show lower activity. The ZrO_2/Cu interface provides the best binding strength.

4.Conclusions

In this paper, a microkinetic model was built to study methanol synthesis on ZrO_2/Cu catalysts. The study tested pressures from 10 to 50 bar. The results show that the catalyst keeps high methanol selectivity (>70%) in this range. However, pure copper makes more CO at high pressures because hydrogen blocks the active sites. The analysis proves that the interface acts as a buffer for carbon species. This effect stops hydrogen from filling the surface. It also lowers the activation energy to 52 kJ mol^{-1}. These results explain the high stability of the catalyst. This finding suggests that increasing the interface area is important for the reaction. However, the model used a static surface. Future work should include surface defects and structural changes to improve accuracy.

References

Boretti, A. (2024). Carbon dioxide hydrogenation for sustainable energy storage. International Journal of Hydrogen Energy, 58, 1386-1395.

Kuterbekov, K. A., Kabyshev, A., Bekmyrza, K., Kubenova, M., Kabdrakhimova, G., & Ayalew, A. T. (2024). Innovative approaches to scaling up hydrogen production and storage for renewable energy integration. International Journal of Low-Carbon Technologies, 19, 2234-2248.

Peng, H., Dong, N., Liao, Y., Tang, Y., & Hu, X. (2024). Real-Time Turbidity Monitoring Using Machine Learning and Environmental Parameter Integration for Scalable Water Quality Management. Journal of Theory and Practice in Engineering and Technology, 1(4), 29-36.

Bagchi, D., Walter, C., Tandava, V. S., Cobos-Becerra, Y. L., Fletcher, J. C., Fischer, N., ... & Menezes, P. W. (2026). Electrochemical Carbon Dioxide Reduction to Methanol on Copper-Based Catalysts: Mechanistic Insights and Industrial Prospects. Advanced Materials, e14994.

Xu, K., Xu, X., Wu, H., & Sun, R. (2024). Venturi Aeration Systems Design and Performance Evaluation in High Density Aquaculture.

Ebrahimian, S., & Bhattacharya, S. (2024). Direct CO 2 Hydrogenation over Bifunctional Catalysts to Produce Dimethyl Ether—A Review. Energies (19961073), 17(15).

Xu, K., Xu, X., Wu, H., Sun, R., & Hong, Y. (2023). Ozonation and Filtration System for Sustainable Treatment of Aquaculture Wastewater in Taizhou City. Innovations in Applied Engineering and Technology, 1-7.

Yang, Z., Kumari, S., Alexandrova, A. N., & Sautet, P. (2025). Catalytic Activity of an Ensemble of Sites for CO2 Hydrogenation to Methanol on a ZrO2-on-Cu Inverse Catalyst. Journal of the American Chemical Society, 147(18), 15294-15306.

Lee, J. D., Qi, Z., Foucher, A. C., Ngan, H. T., Dennis, K., Cui, J., ... & Biener, J. (2022). Facilitating hydrogen dissociation over dilute nanoporous Ti–Cu catalysts. Journal of the American Chemical Society, 144(37), 16778-16791.

Ghoshal, S., Roy, P., Pramanik, A., & Sarkar, P. (2022). Ru/Rh catalyzed selective hydrogenation of CO 2 to formic acid: a first principles microkinetics analysis. Catalysis Science & Technology, 12(23), 7219-7232.

Wang, Y., Wang, Y., Yin, X., Arias, R., & Chen, J. (2026). Research on Dynamic Assessment of Glucose-Lipid Metabolism and Personalized Drug Response Prediction Based on Wearable Multimodal Sensing.

Rommens, K. T., & Saeys, M. (2023). Molecular views on Fischer–Tropsch synthesis. Chemical Reviews, 123(9), 5798-5858.

Dhakshinamoorthy, A., Navalón, S., Primo, A., & García, H. (2024). Selective gas-phase hydrogenation of CO2 to methanol catalysed by metal-organic frameworks. Angewandte Chemie, 136(3), e202311241.

Wang, C., & Chakrapani, V. (2023). Photocatalytic generation of reactive oxygen species on Fe and Mn oxide minerals: mechanistic pathways and influence of semiconducting properties. The Journal of Physical Chemistry C, 127(48), 23189-23198.

Margraf, J. T., Jung, H., Scheurer, C., & Reuter, K. (2023). Exploring catalytic reaction networks with machine learning. Nature Catalysis, 6(2), 112-121.

Wang, C., & Chakrapani, V. (2023). Environmental Factors Controlling the Electronic Properties and Oxidative Activities of Birnessite Minerals. ACS Earth and Space Chemistry, 7(4), 774-787.

Ganti, S. S. S., Roy, P. K., Wagh, N., Sai, K. N. S. S., & Kumar, S. (2025). Strategically designed catalysts for ammonia synthesis under mild conditions: recent advances and challenges. Journal of Materials Chemistry A.

Ebrahimi, P., Kumar, A., & Khraisheh, M. (2022). A review of CeO2 supported catalysts for CO2 reduction to CO through the reverse water gas shift reaction. Catalysts, 12(10), 1101.